Supporting Information for "The effect of Small Scale Soil Heterogeneity on conservative Transport: the Key Role of (Spatially Variable) Diffusion"

Christopher V. Henri[1], Efstathios Diamantopoulos[2]

[1]Geological Survey of Denmark and Greenland, Copenhagen, Denmark

[2]Department of Plant and Environmental Sciences, University of Copenhagen, Copenhagen, Denmark

Contents of this file

1. Figures S1 to S11

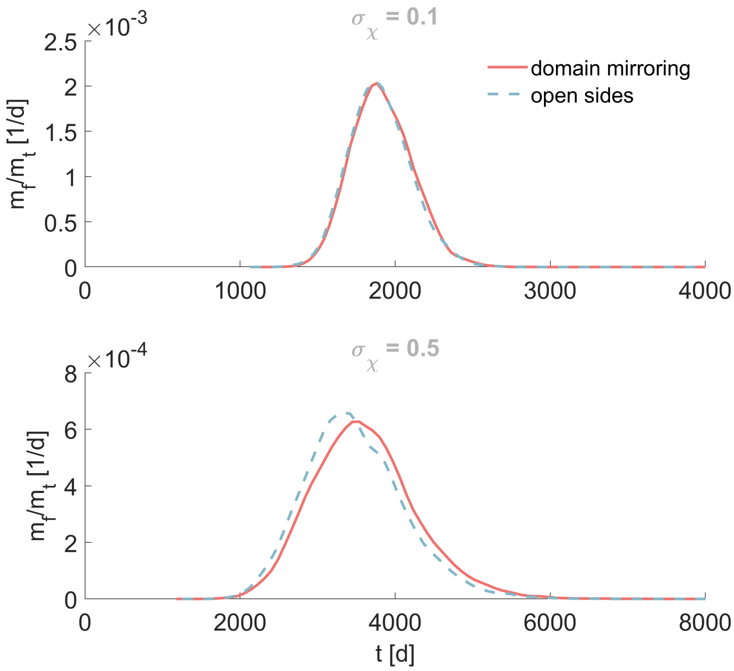

Figure S1. Mass fluxes (normalized by the total mass reaching the bottom of the domain) temporal evolution for a low (top) and high (bottom) degree of heterogeneity if particles are allowed to leave the sides of the domain (dashed blue line) and if particles are transferred to the opposite side of domain (plain red line). BTCs are shown for a low flux (diffusion dominated scenario).

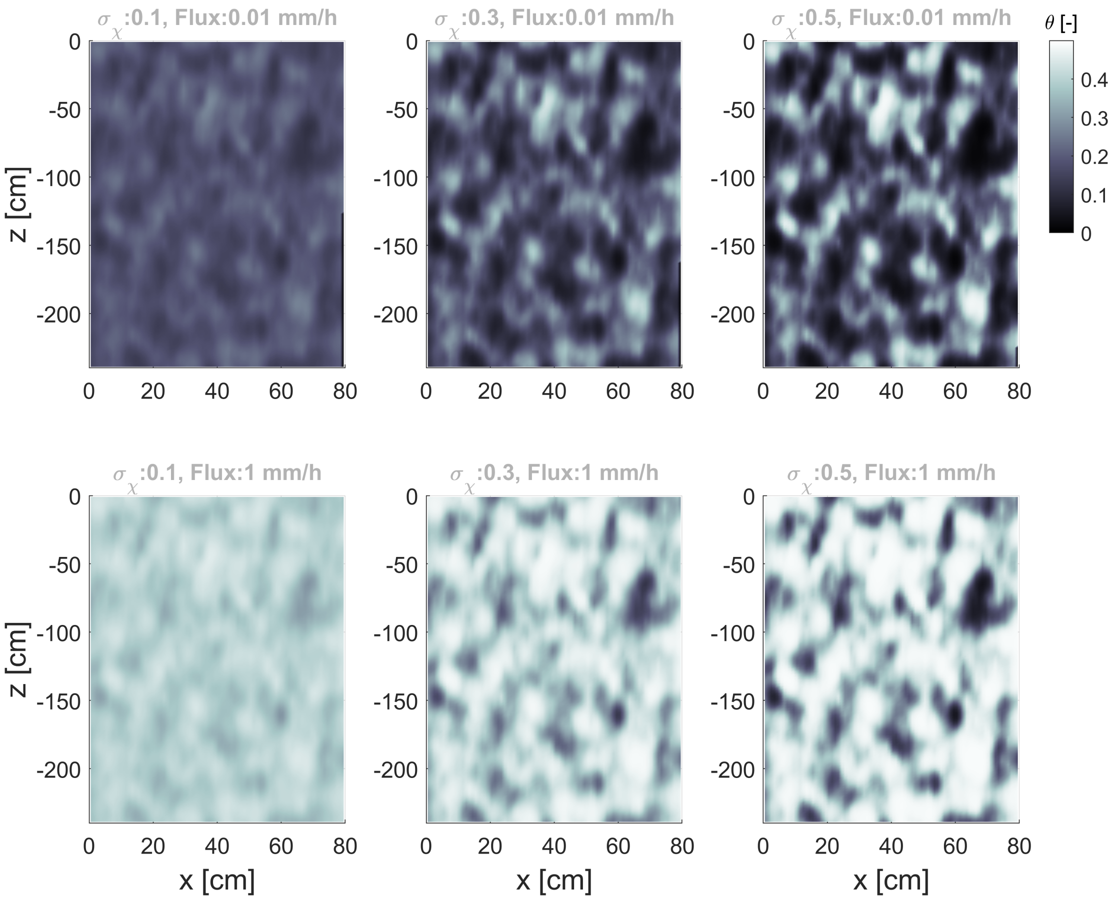

Figure S2. Resulting spatial distribution of the water content (θ) for each degree of soil heterogeneity and for a high recharge flux (top frames) and a low recharge flux (bottom frames).

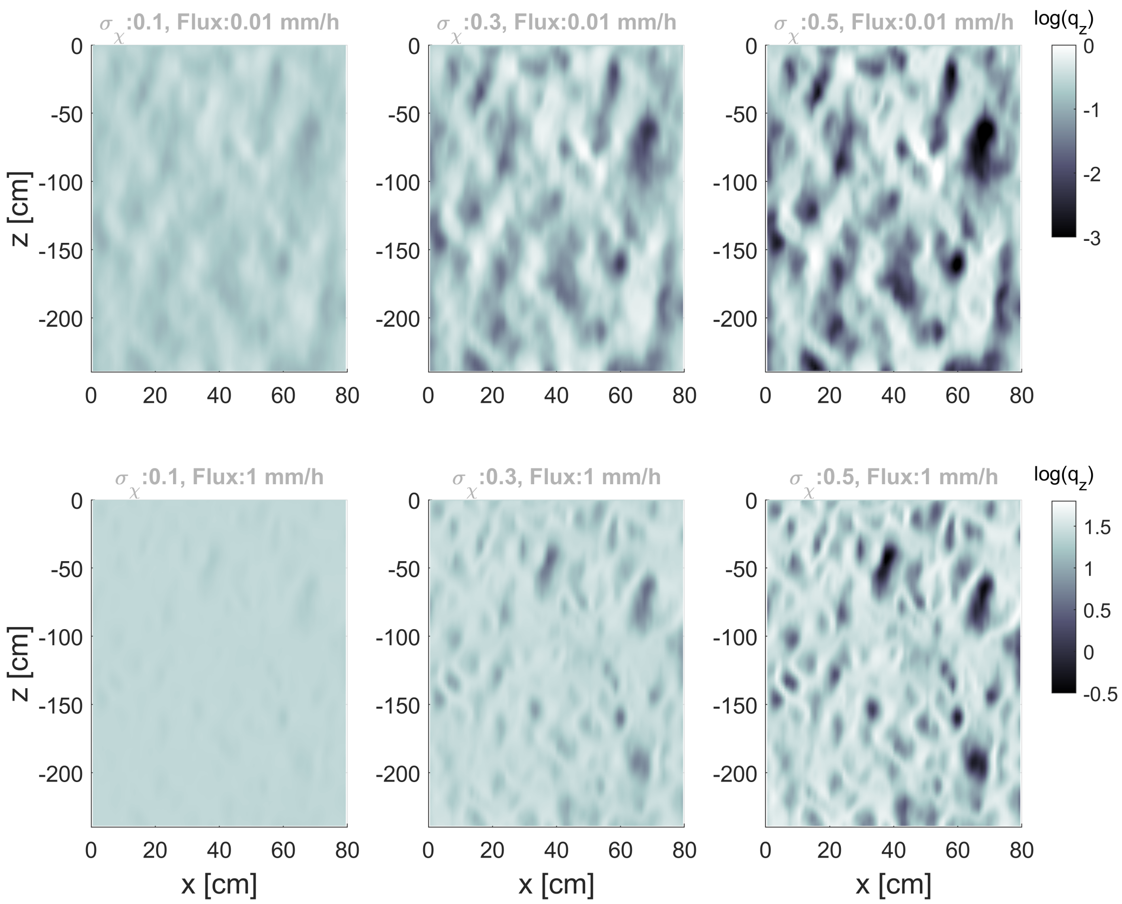

Figure S3. Resulting spatial distribution of the (logarithm of the) vertical Darcy flux (qz) for each degree of soil heterogeneity and for a high recharge flux (top frames) and a low recharge flux (bottom frames).

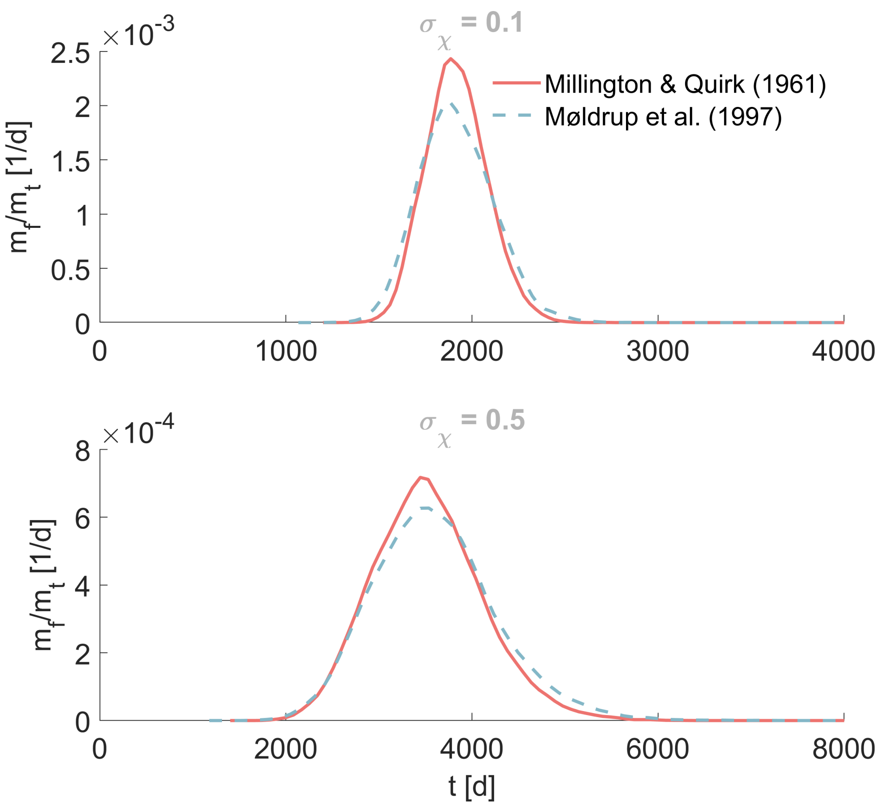

Figure S4. Mass fluxes temporal evolution for a low (top) and high (bottom) degree of heterogeneity if the Millington's model of tortuosity is used (plain red line) and if the Moldrup's model of tortuosity is used (dashed blue line). BTCs are shown for a low flux (diffusion dominated scenario) and the highest degree of heterogeneity.

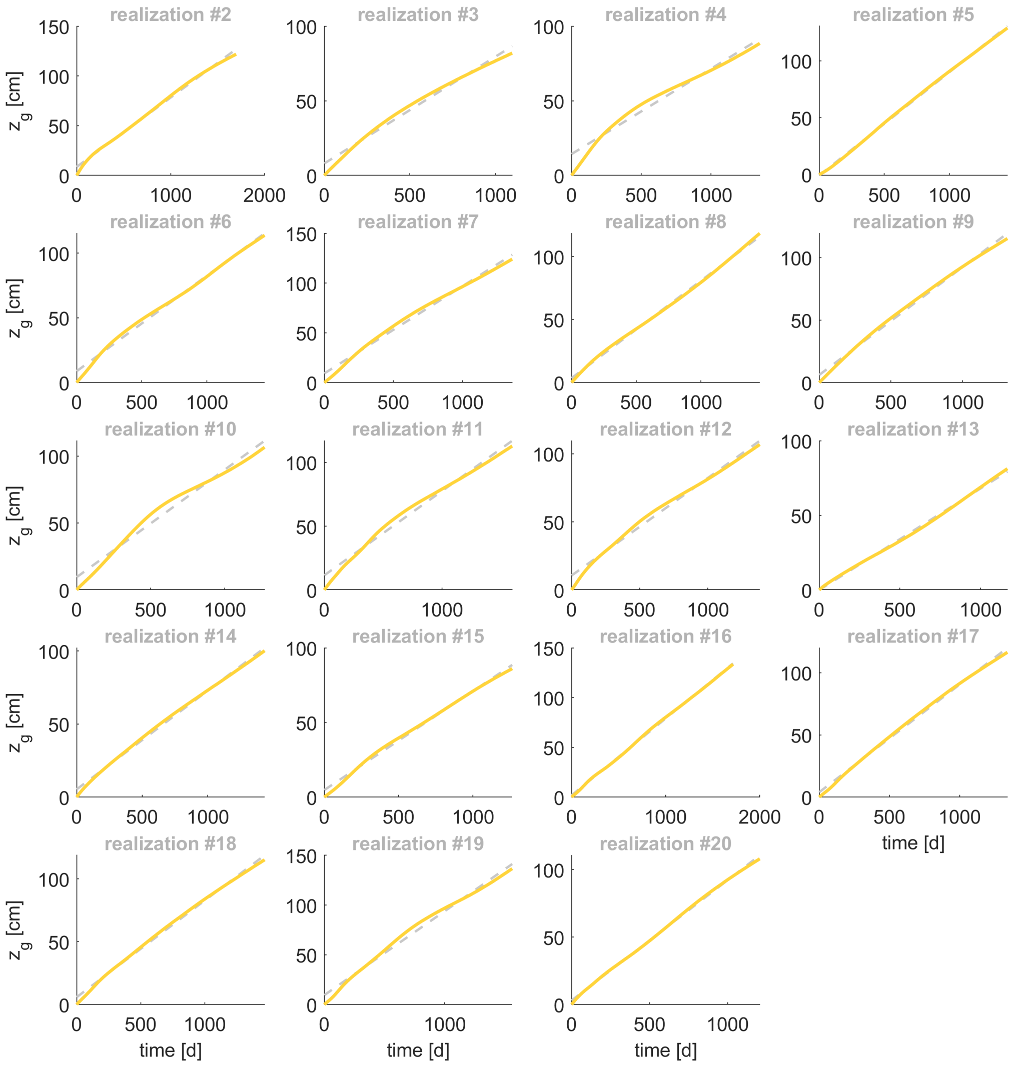

Figure S5. First spatial moment (Y_g) temportal evolution for all realizations. Results are shown for a low flux and the highest degree of heterogeneity.

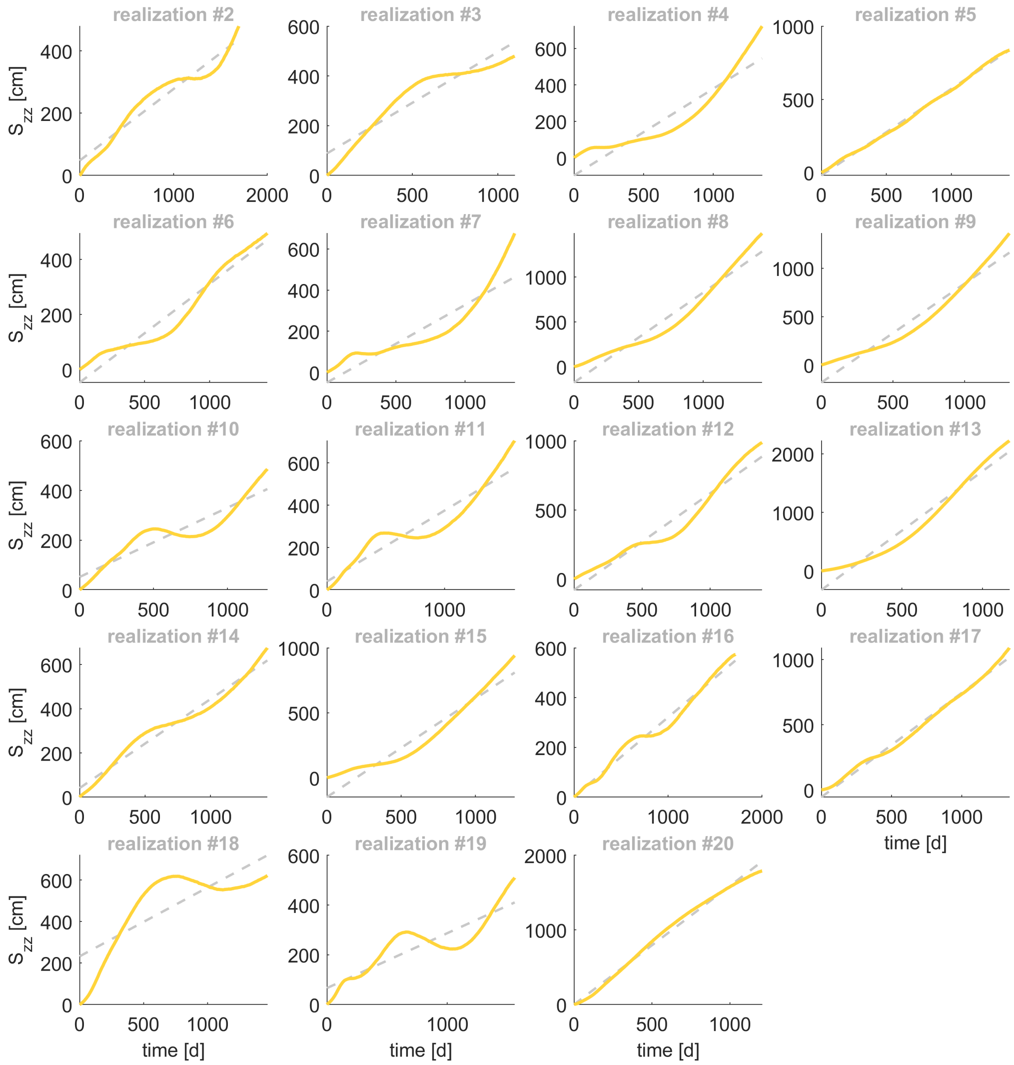

Figure S6. Second spatial moment (S_{zz}) temportal evolution for all realizations. Results are shown for a low flux and the highest degree of heterogeneity.

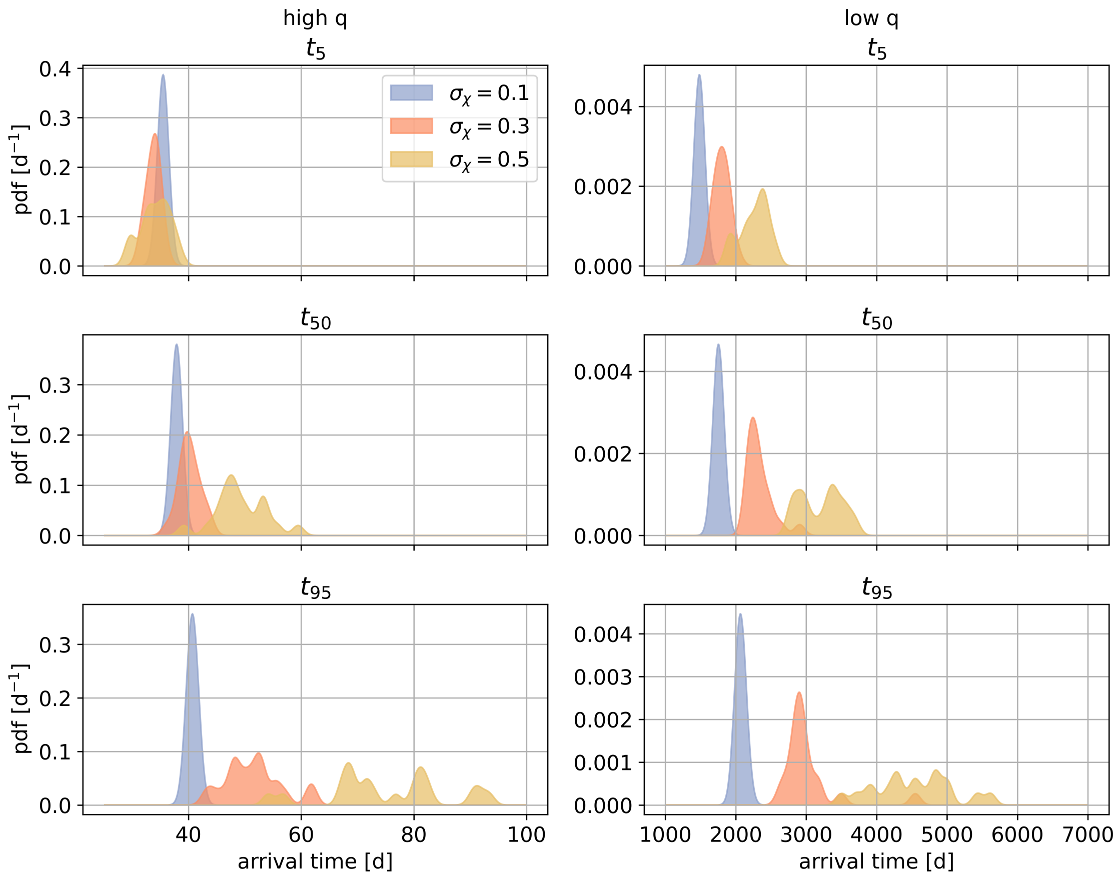

Figure S7. Probability density functions of the arrival time of 5 (top frames), 50 (middle frames) and 95% (bottom frames) of the total injected mass for each flow and heterogeneity scenario. The diffusion coefficient is considered spatially variable (tortuosity dependent).

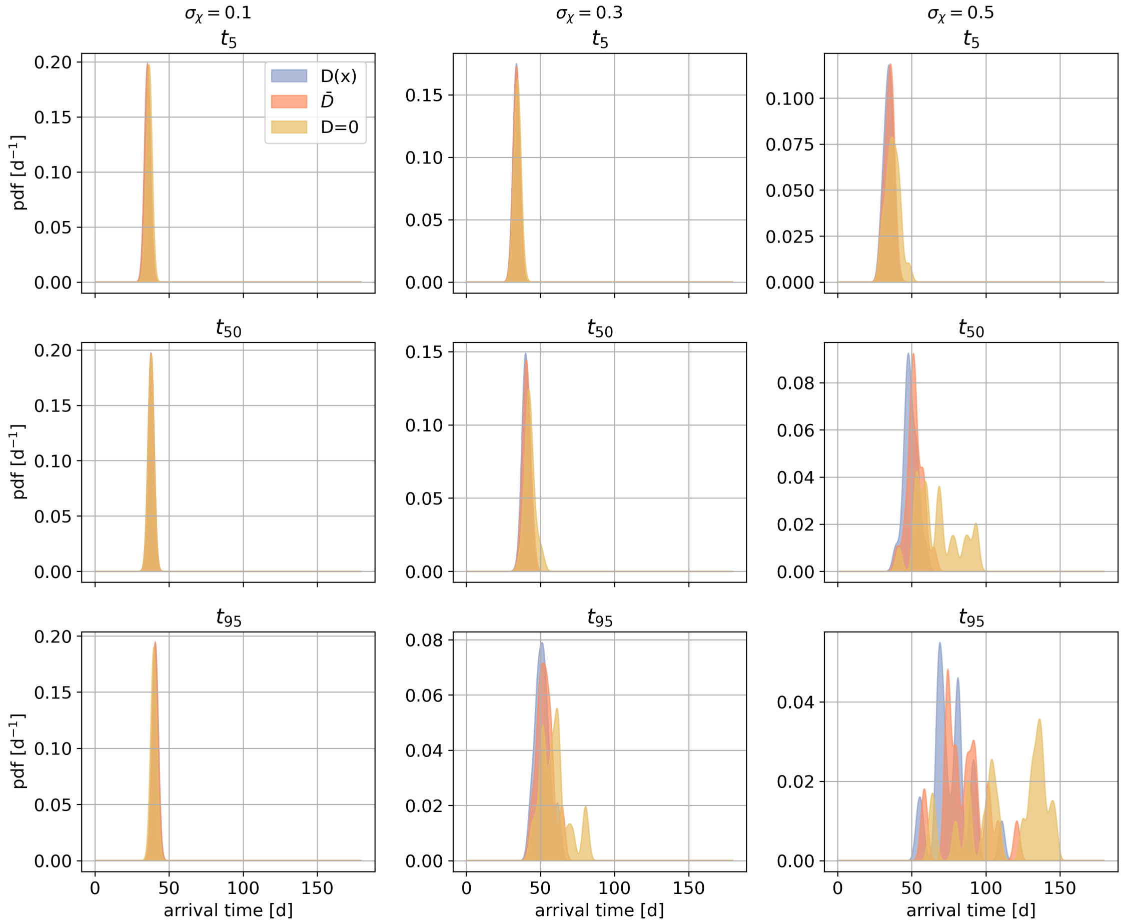

Figure S8. Probability density functions of the arrival time of 5 (top frames), 50 (middle frames) and 95% (bottom frames) of the total injected mass for each heterogeneity scenario and diffusion model. Results are shown for the higher Peclet number.

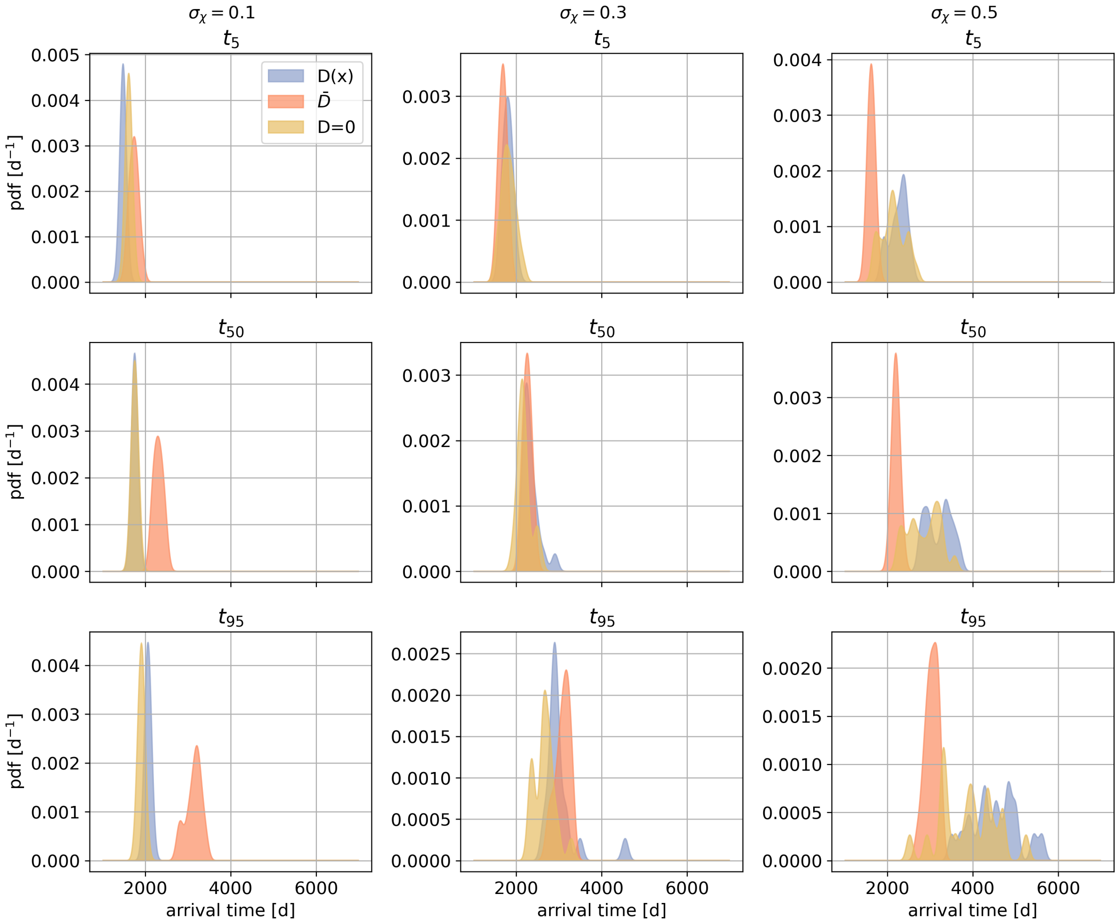

Figure S9. Probability density functions of the arrival time of 5 (top frames), 50 (middle frames) and 95% (bottom frames) of the total injected mass for each heterogeneity scenario and diffusion model. Results are shown for the lower Peclet number.

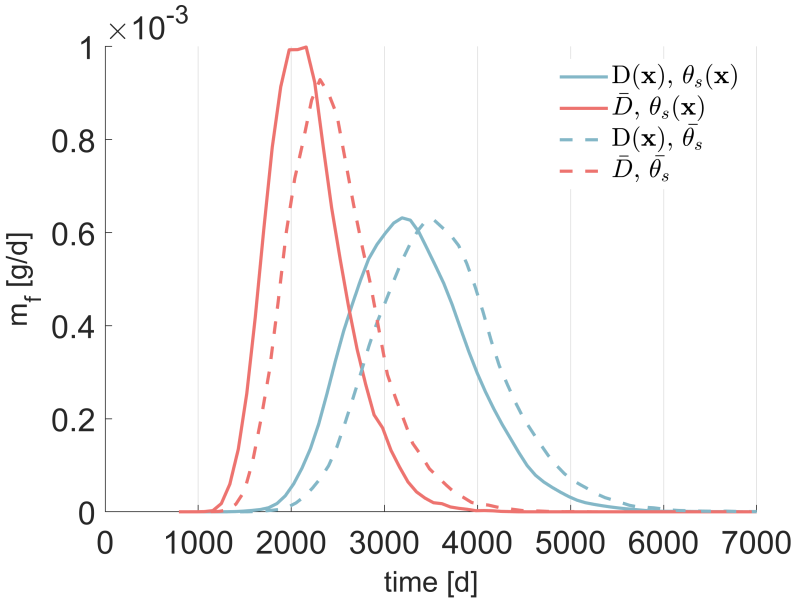

Figure S10. Mass fluxes temporal evolution for a spatially variable diffusion coefficient ($D(x)$, blue lines) or a homogeneous, averaged diffusion coefficient ($\bar{D}$, red lines) and for a spatially variable saturated water content ($\theta_s(x)$) or a homogeneous, averaged saturated water content ($\bar{\theta}_s$). BTCs are shown for a high degree of heterogeneity ($\sigma_\chi = 0.5$) and a low flux (diffusion dominated scenario).

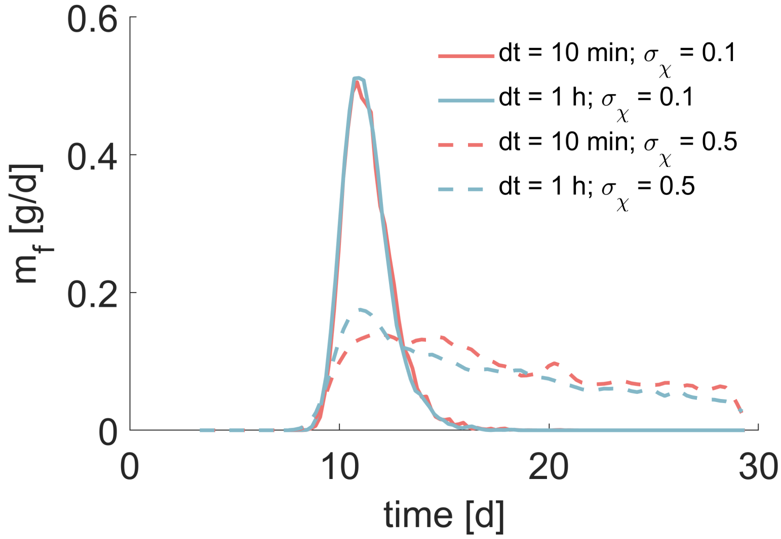

Figure S11. Mass fluxes temporal evolution for a low (plain lines) and high (dashed lines) degree of heterogeneity for 2 temporal discretization of the Darcy fluxes and the water content used in to solve the transport problem. *CP 80 cm; 10 days of infiltration*